Journal of the Mechanical Behavior of Biomedical Materials 80 (2018) 303–310

Contents lists available at ScienceDirect

Journal of the Mechanical Behavior of Biomedical Materials

journal homepage: www.elsevier.com/locate/jmbbm

Adhesion and relaxation of a soft elastomer on surfaces with skin like roughness

Sarah C.L. Fischer[a,b], Silviya Boyadzhieva[a,b], René Hensel[a], Klaus Kruttwig[a], Eduard Arzt[a,b,*]

[a] INM – Leibniz Institute for New Materials, Campus D2 2, Saarbrücken, Germany
[b] Department of Materials Science and Engineering, Saarland University, Campus D2 2, Saarbrücken, Germany

ABSTRACT

For designing new skin adhesives, the complex mechanical interaction of soft elastomers with surfaces of various roughnesses needs to be better understood. We systematically studied the effects of a wide set of roughness characteristics, film thickness, hold time and material relaxation on the adhesive behaviour of the silicone elastomer SSA 7–9800 (Dow Corning). As model surfaces, we used epoxy replicas obtained from substrates with roughness ranging from very smooth to skin-like. Our results demonstrate that films of thin and intermediate thickness (60 and 160 μm) adhered best to a sub-micron rough surface, with a pull-off stress of about 50 kPa. Significant variations in pull-off stress and detachment mechanism with roughness and hold time were found. In contrast, 320 μm thick films adhered with lower pull-off stress of about 17 kPa, but were less sensitive to roughness and hold time. It is demonstrated that the adhesion performance of the silicone films to rough surfaces can be tuned by tailoring the film thickness and contact time.

1. Introduction

The surface and contact topography strongly affects the adhesive interaction between two materials (Fuller and Tabor, 1975; Briggs and Briscoe, 1977; Barreau et al., 2016). It is well recognized that the adhesion to rough surfaces is reduced due to the absence of full surface contact (Greenwood and Williamson, 1966; Persson and Tosatti, 2001; Dapp et al., 2012; Putignano et al., 2015). Several parameters, such as compressive preload and hold time as well as film thickness and mechanical properties, influence the adhesive behaviour (Fuller and Tabor, 1975; Davis et al., 2014, 2012; Purtov et al., 2013). Only a few systematic adhesion studies exist on surfaces exhibiting roughness in the micron range. Especially contact time and relaxation of the adhesive materials are factors whose influence needs to be better understood. Roughness, material properties and the thickness of the adhesive material notably affect the detachment mechanism from the surface (Davis et al., 2012; Fischer et al., 2017a; Nase et al., 2008). While edge cracks often yield unstable, spontaneous detachment, other mechanisms including cavitation in the interior of the contact area and specifically center cracks can result in stable crack growth and thus can increase the work of separation and the pull-off strength (Davis et al., 2014; Fischer et al., 2017a; Nase et al., 2008; Lakrout et al., 1999).

Skin is an example of a particularly complex, rough surface with properties depending on several factors including humidity, secretion, environmental conditions and the presence of skin care products (Tang et al., 2015; Tobin, 2006). Adhesion to skin is needed for wound dressings or for emerging consumer applications, e.g. wearable electronic devices and activity trackers (Venkatraman and Gale, 1998; Kim et al., 2016; Laulicht et al., 2012). The adhesive performance of skin dressings is often characterized by peel or tack tests on substitute materials such as stainless steel or polycarbonate substrates, both exhibiting nanoscopic or sub-micron roughness (Krueger et al., 2013; Wokovich et al., 2008). For the development and improvement of innovative skin adhesives, a fundamental understanding of the material interaction with surfaces exhibiting skin-like roughness is necessary. Standardized measurements are complicated by the fact that human skin exhibits mean peak-to-valley distances in the range of 50–70 μm depending on age and location on the body surface (Quan et al., 1997). Because these variations influence measurements significantly, skin substitutes composed of synthetic and natural materials have been evaluated (Jones et al., 2002; Netzlaff et al., 2005; Renvoise et al., 2009). The surface free energy of human skin has been reported to be between 38 and 57 mJ/m^2, depending on temperature and humidity (Kenney et al., 1992) and therefore differs significantly from 500 mJ/m^2, the surface free energy which has been reported for stainless steel (Wokovich et al., 2008). Surface free energies of about 30 mJ/m^2 have been reported for cured epoxy resins and therefore match human skin properties exceptionally well (Castellanos et al., 2011). In addition,

* Corresponding author at: INM – Leibniz Institute for New Materials, Campus D2 2, Saarbrücken, Germany.
E-mail address: eduard.arzt@leibniz-inm.de (E. Arzt).

https://doi.org/10.1016/j.jmbbm.2018.01.032
Received 2 November 2017; Received in revised form 26 January 2018; Accepted 28 January 2018
Available online 31 January 2018

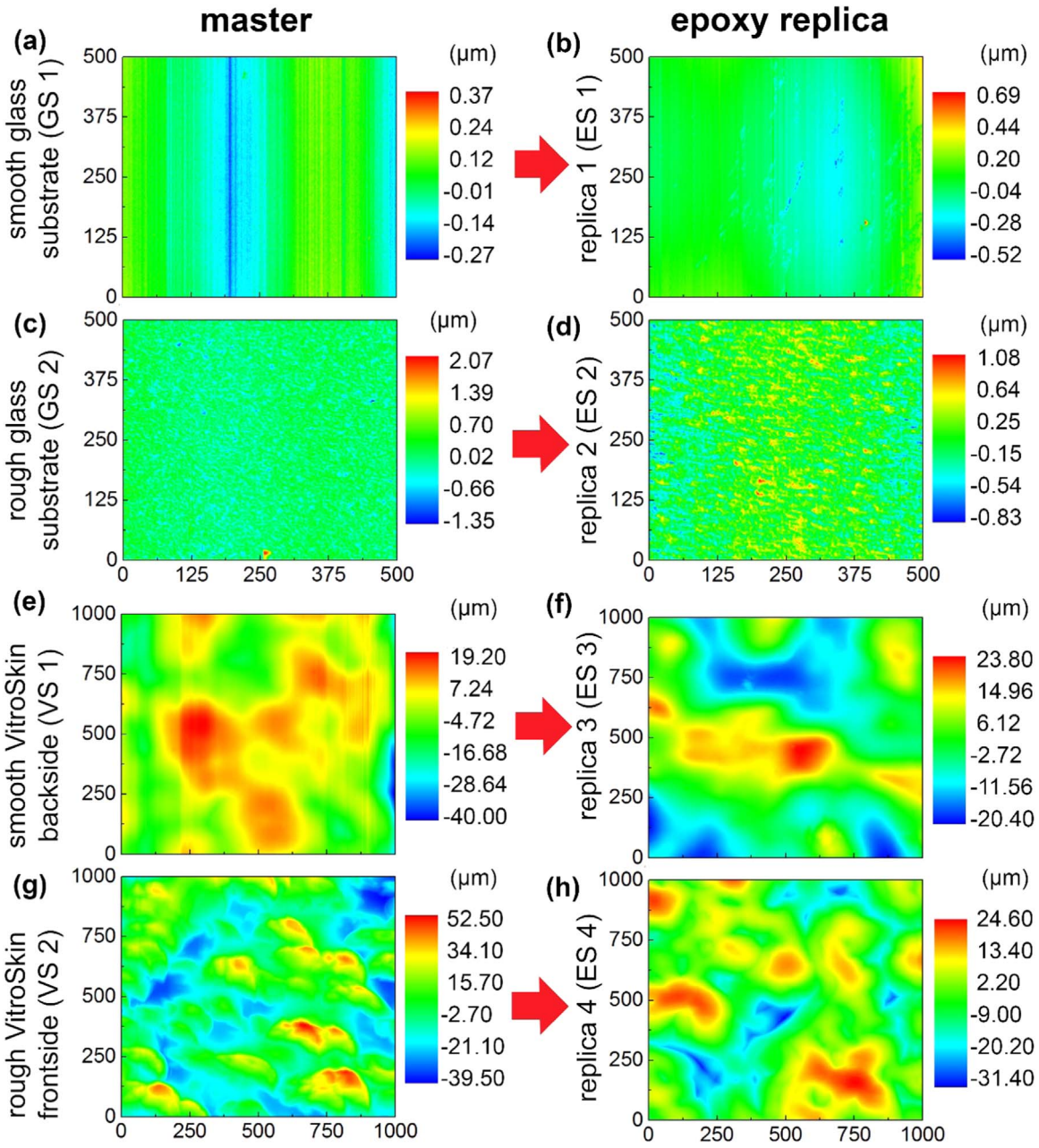

Fig. 1. Topography of substrates used for adhesion testing, as characterized by stylus profilometry. (a)–(d) glass substrates (GS 1 and GS 2) and their epoxy replicas (ES 1 and ES 2), scans of 500 × 500 μm. (e)–(h) VitroSkin substrates (VS 1 and VS 2) and their epoxy replicas (ES 3 and ES 4), scans of 1000 × 1000 μm. Due to the large roughness range, the roughness scales differ.

epoxy molding has been performed in all cases to keep the surface free energy constant, allowing us to overcome effects related to the different surface free energies associated with glass and Vitroskin.

In previous work, we analysed the mechanical properties, adhesion properties and biocompatibility of the soft skin adhesive SSA MG 7–9800 (SSA, Dow Corning, Auburn, MI, USA) and Sylgard 184 (Dow Corning, Auburn, MI, USA). Their applicability to biomedical applications was studied as a function of the mixing ratio of the base to crosslinker of the two-component systems (Fischer et al., 2017b). In these investigations we limited our study to glass substrates with low roughness (R_z = 0.04 to 2.2 μm) and a restricted range of film thicknesses (50–230 μm). The pull-off strength was found to increase with decreasing film thickness and increasing elastic modulus on the smooth substrate, and significantly decreased on the rough glass substrate except for SSA in the mixing ratio 1:1.

The present paper provides comprehensive insight into the effects of film thickness and surface roughness on the adhesion of the silicone adhesive SSA MG 7–9800. Parameters included film thickness (from 60 to 320 μm), substrate roughness (R_z from 0.1 to 84.2 μm) and hold time (from 1 to 300 s). Surface roughness comparable to skin was produced by replicating epoxy resins from glass surfaces or from the artificial skin model VitroSkin (Chen and Bhushan, 2013). VitroSkin has been shown to exhibit mechanical properties and surface roughness comparable to animal skin (Chen and Bhushan, 2013; Lir et al., 2007). From the results, we conclude that two different regimes are present, fundamentally affecting the adhesive behaviour: a roughness insensitive regime when the film thickness is higher than the material-specific critical roughness parameter and a roughness sensitive regime in the other case.

2. Materials and methods

2.1. Manufacturing of adhesive film samples

Polymer films were manufactured from SSA MG 7–9800 (Dow Corning, Auburn, MI, USA) in a mixing ratio of 1:1 wt parts by a doctor blade technique with an automatic thin film applicator (AFA-IV, MTI Corporation, Richmond, CA, USA). After deposition on glass, the films were cured at 95 °C for one hour. The film thickness was measured by optical microscopy (Keyence, Osaka, Japan). Thickness values were 60 ± 10 μm (denoted as "thin"), 160 ± 25 μm ("medium") and 320 ± 30 μm ("thick"). The samples were prepared on glass plates with an area of about 7x20 cm^2, and subsequently cut into samples of about 4 cm^2 for adhesion testing.

2.2. Adhesion measurements and analysis

Adhesion measurements were performed using a custom-built setup as described previously (Fischer et al., 2017b). The approach and retraction velocity were set to 30μm/s and 10μm/s, respectively. The hold time, t_{hold}, was varied from 1 to 300 s. The compressive preload stress, σ_0, was kept constant at 10 ± 3 kPa. Measurements were performed with at least four independent adhesive films and at three different locations on each surface.

From the measured values of the force, F, and the displacement, s, we calculated the stress, $\sigma = F/A$, where A is the nominal contact area (about 7 mm^2 for the epoxy substrates). The relative displacement was defined as $\varepsilon = (s-s_0)/h_{film}$, where h_{film} is the film thickness and s_0 the displacement at force zero. To analyse and compare the adhesive behaviour, three parameters were chosen: the maximum pull-off stress, σ_{max}; the maximum relative displacement, ε_{max}; and the work of separation, $W_{sep} = \int_{s_0}^{s_{end}} \sigma ds$ where s_{end} is the displacement at which complete detachment occurred.

2.3. Substrate manufacturing

Substrates of different materials and surface roughness were used (cf. Fig. 1 and Fig. 2). The reference substrates consisted of a polished glass slide (denominated as GS 1, area $A = 3.2\ mm^2$) (Hellma Optik GmbH, Jena, Germany), frosted glass (GS 2, $A = 6.7\ mm^2$)) (Marienfeld, Lauda Königshofen, Germany), VitroSkin (IMS inc., Portland, ME, USA) backside (VS 1, $A = 7.6\ mm^2$) and VitroSkin frontside (VS 2, $A = 7.6\ mm^2$). While for GS 1 the glass was purchased as a cylinder with 2 mm diameter, a circular substrate with about 3 mm diameter was machined out of a frosted glass slide for GS 2. For the VitroSkin, circular substrates with about 3 mm diameter were extracted using a biopsy punch (Integra Miltex Inc., York, PA, USA).

Epoxy substrates were replicated from different master substrates: a regular glass slide (ES 1, $A = 6.1\ mm^2$) (Marienfeld, Lauda Königshofen, Germany), a frosted glass slide (ES 2, $A = 7.0\ mm^2$) (Marienfeld, Lauda Königshofen, Germany), VitroSkin (IMS inc., Portland, ME, USA) backside (ES 3, $A = 7.1\ mm^2$) and VitroSkin frontside (ES 4, $A = 7.2\ mm^2$). The epoxy resin (Résine epoxy R123, Soloplast-Vosschemie, Fontanil-Cornillon, France) was mixed in 100:45 wt ratio of base to curing agent as specified by the supplier, cured on the respective substrate at room temperature for over 12 h and then extracted with a biopsy punch of 3 mm diameter.

All substrates were attached to an aluminium mount compatible with our adhesion setup using UV adhesive (Bohle Ltd., Cheshire, UK), for GS 1–2 and ES 1–4, or epoxy resin, for VS 1–2. The displacements measured during the tests were corrected for the system compliance $C = 0.12$ μm/mN for glass and $C = 0.13$ μm/mN for epoxy and VitroSkin.

2.4. Substrate characterization

The exact nominal area of each substrate was measured using optical microscopy (Keyence, Osaka, Japan) and used in the stress calculations. Their roughness parameters were measured by stylus profilometry (Surfcom 1500SD3, Carl Zeiss, Oberkochen, Germany). Roughness power spectra were determined using the Surface Topography Analyzer developed by Lars Pastewka (http://contact.engineering/) (Jacobs et al., 2017).

3. Results

In this section, we first present the results of the substrate surface characterization. Subsequently, the results of the adhesion test with the different adhesive samples are reported as a function of film thickness, surface roughness and hold time.

3.1. Substrate surfaces

Fig. 1 and Fig. 2 show the results of the substrate surface characterization. As can be seen, the replication process led to slight differences in the topographies between master and replica. From the table in Fig. 2 we can see that, except for ES 3, the roughness parameters R_a and R_z seem to slightly decrease after replication. Fig. 2 reveals also slight differences between the respective power spectra. The power spectra of the glass and the VitroSkin substrates have

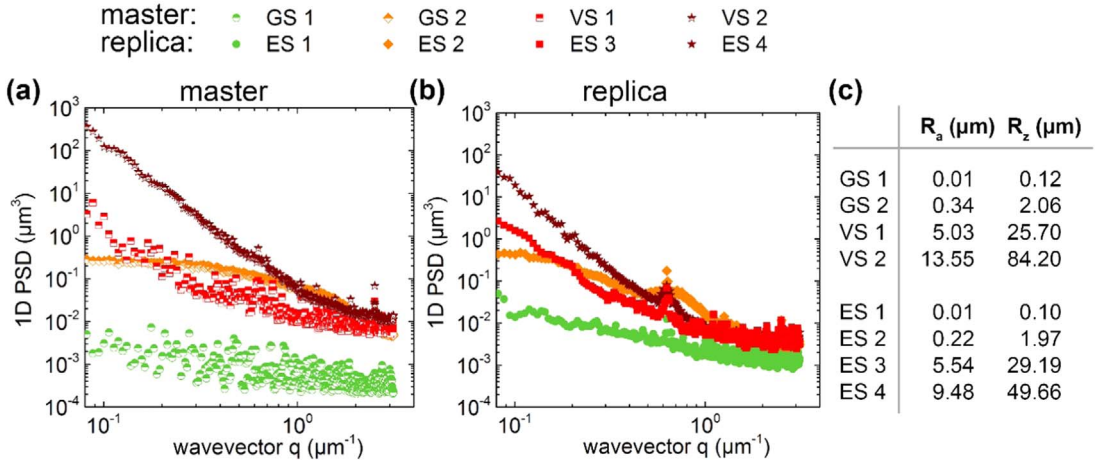

(c)

	R_a (μm)	R_z (μm)
GS 1	0.01	0.12
GS 2	0.34	2.06
VS 1	5.03	25.70
VS 2	13.55	84.20
ES 1	0.01	0.10
ES 2	0.22	1.97
ES 3	5.54	29.19
ES 4	9.48	49.66

Fig. 2. Roughness power spectra of the substrates used for adhesion testing. 1D power spectra of (a) the glass and VitroSkin master surfaces (GS 1–2; VS 1–2) and (b) the epoxy replica (ES 1–4) based on profilometer scans and generated with the Surface Topography Analyzer (http://contact.engineering/) (Jacobs et al., 2017). (c) Resulting roughness parameters of all surfaces: average roughness R_a and average peak-to-valley distance R_z.

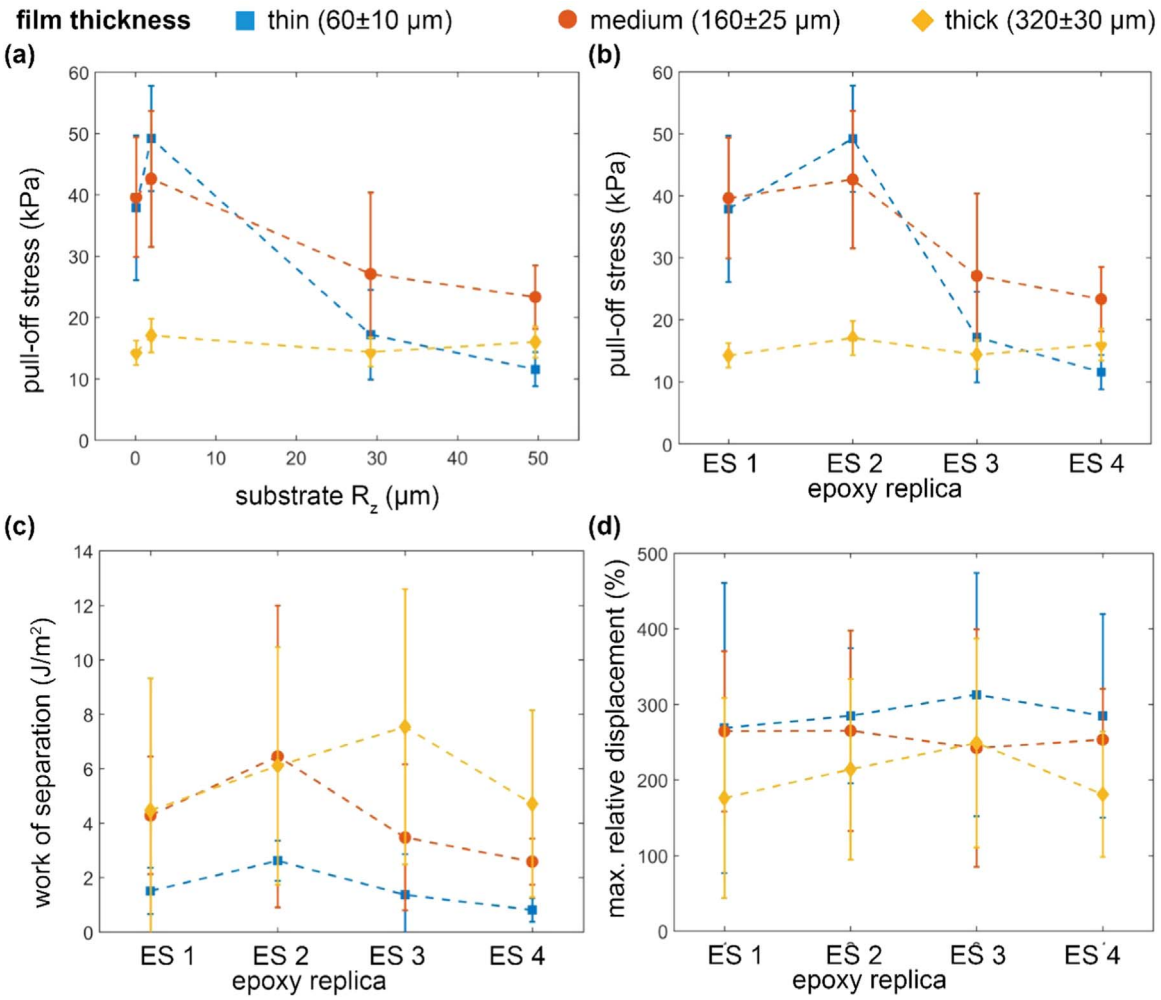

Fig. 3. Adhesion measurement results as function of film thickness and substrate roughness. (a) Pull-off stress as a function of the roughness parameter R_z and (b) pull-off stress, (c) work of separation and (d) maximum relative displacement for the films with three different thickness on four epoxy substrates. The hold time was 1 s.

considerably different slopes and thus height distributions.

3.2. Influence of film thickness and roughness

Fig. 3 depicts the adhesion parameters measured, with a hold time of 1 s, for the different film thicknesses and substrate topographies. Each data point corresponds to the average of about twelve measurements, corresponding to at least four independent adhesive films with three positions on each film. The "thick" films exhibited similarly low pull-off stresses on all four substrates of about 17 kPa (Figs. 3**a** and 3**b**). The "medium" and "thin" films, in contrast, showed a dependence of the pull-off stress on the substrate. Within the error bars, the behaviour of the two films on glass was virtually indistinguishable (Fig. 3**a**); the adhesion to the smoothest substrate ES 1 was about 40 kPa and, interestingly, seemed to increase for the rougher ES 2 substrate to between 40 and 50 kPa. It is debatable whether this increase is statistically significant in view of the error margins, a point that will be discussed below. On the roughest substrates (ES 3 and ES 4), the pull-off stress decreased substantially, with the "thin" film showing a stronger decrease.

The work of separation was found to be lowest for the "thin" films, with values of about 2 J/m^2 and a slight maximum of 2.5 J/m^2 for ES 2 (Fig. 3**c**). The "medium" and "thick" films displayed almost twice this value and are again virtually indistinguishable within the error margins. A small, probably insignificant variation for the different substrates could be observed, with maximum values of 6.5 J/m^2 and 7.5 J/m^2 for substrates ES 2 and ES 3, respectively. The maximum relative displacement observed for all three films on all four substrates was, within the error margin, of similar magnitude between 180% and 300% (Fig. 3**d**).

In addition to quantitative differences, the detachment mechanisms of the films varied depending on film thickness and substrate roughness (Fig. 4). Finger-like cracks originating from the contact edge were observed in all cases, with dimensions increasing with increasing film thickness. Thus, in thinner films, the fingers were finer than in thicker films. On the smoothest substrate, cavitation in the interior of the contact area were exclusively seen in thinner films. Increasing the surface roughness led to augmented occurrence of cavitation in the medium and thick films. These differences influenced the adhesion strength on the different substrates as described quantitatively before.

3.3. Influence of hold time and material relaxation

Viscoelastic materials exhibit time-dependent stress relaxation during a hold time at constant displacement (Fischer et al., 2017a). The compressive stress σ as a function of time t can be approximated by the following equation based on the Kelvin model: (Findley et al., 2013; Ferry, 1980; Tirella et al., 2014)

$$\sigma = \sigma_\infty + \sigma_1 \cdot exp\,(-t/\tau_1) + \sigma_2 \cdot exp\,(-t/\tau_2), \quad (1)$$

where σ_1 and σ_2 are stress constants and τ_1 and τ_2 are time constants, and σ_∞ is the stress value for infinite hold time ($t \to \infty$). The initial stress,

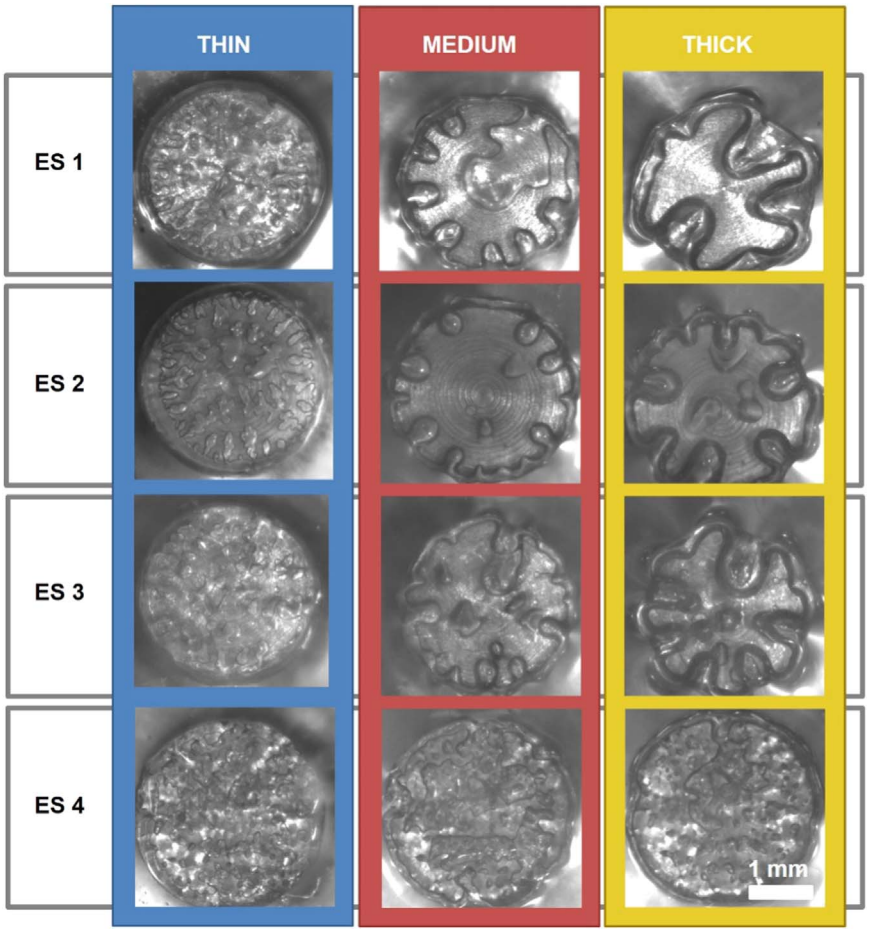

Fig. 4. Exemplary pictures of the detachment mechanisms. Debonding of a "thin" (blue), "medium" (red) and "thick" (yellow) film from the epoxy substrates with increasing surface roughness. Finger-like cracks originating from the contact edge are observed in all cases. In thicker films, the fingers are coarser than in thinner films. Additional crack formation in the interior of the contact (cavitation) is seen in thinner films, especially in contact with substrates of higher roughness.

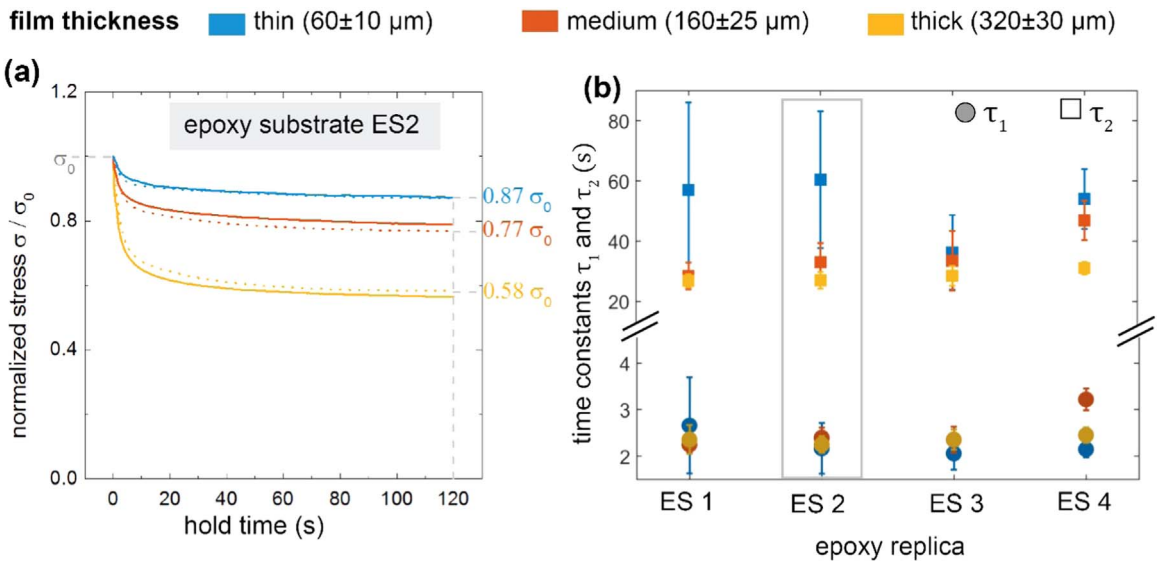

Fig. 5. Stress relaxation behaviour of the films on the different substrates. (a) Stress, normalized by the compressive pre-stress σ_0 of about 10 kPa, vs. hold time. Data shown are for the epoxy replica ES 2. Dots are experimental data, lines represents fits to Eq. (1). The values right to the curves represent the stress decreases at 120 s contact time relative to the initial pre-stress. (b) Time constants τ_1 (circles) and τ_2 (squares) obtained as a function of substrate and film thickness (see color code).

denoted as σ_0, is given by $\sigma_\infty + \sigma_1 + \sigma_2$. For $\tau_1 < \tau_2$,the short time relaxation behaviour is described by τ_1 and σ_1, whereas τ_2 and σ_2 describes the long-term behaviour. By fitting the parameters σ_∞, σ_1, σ_2, τ_1, and τ_2, the stress relaxation during 120 s hold time at an initial pre-stress of 10 ± 2 kPa was reproduced in Fig. 5 and Supplementary Fig. S2 (all fit parameters can be found in the Supplementary Table ST1).

Fig. 5**a** shows that the normalized stress relaxation was higher for "thick" films, with a stress drop of 42% after 120 s compared to only 23% for the "thin" films. For all films, the stress at 120 s hold time was already very close to the estimated stress, σ_∞, at infinite contact times (see Supplementary Table ST1), which means that the material relaxation is close to saturation after 120 s. The relaxation time τ_1 was

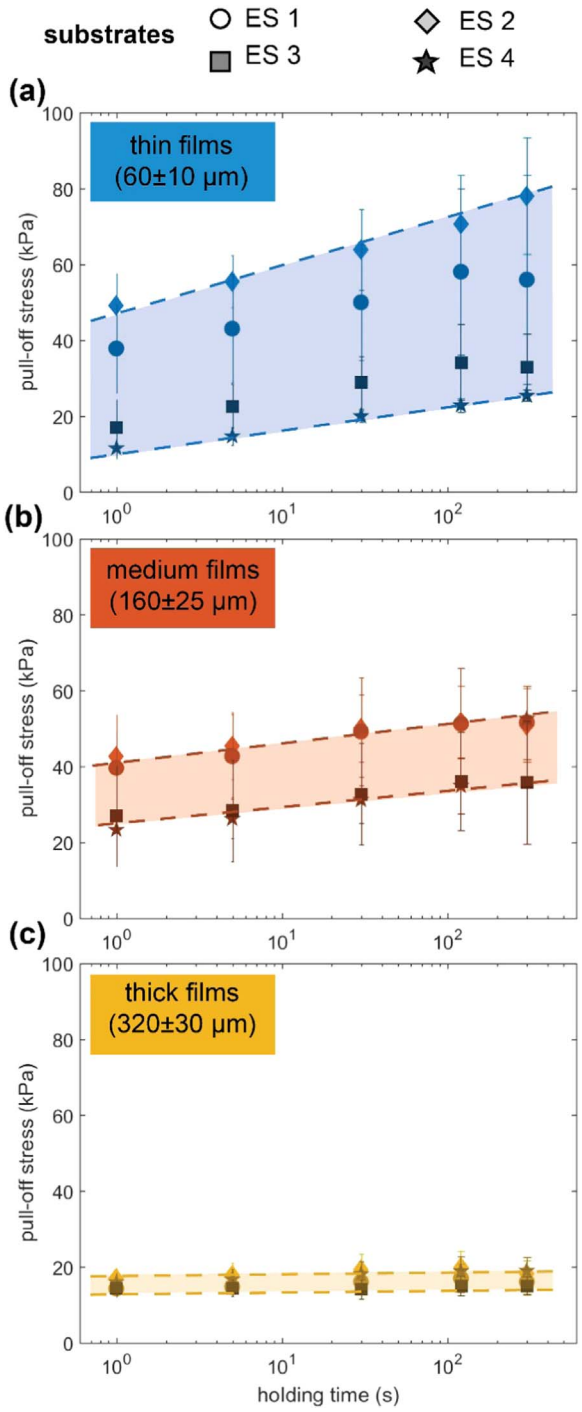

Fig. 6. Hold time effect on adhesion: Pull-off stress as a function of hold time for (a) thin (60 ± 10 µm), (b) medium (160 ± 25 µm) and (c) thick films (320 ± 30 µm) on the different epoxy substrates. The dashed lines are intended to guide the eye of the reader.

similar for all film thicknesses and substrates with a value of about 2.4 ± 0.3 s (Fig. 5**b**). The relaxation time τ_2 varied with film thickness and substrate roughness: for the "medium" and the "thick" films, τ_2 slightly increased with roughness (from 28 ± 4 s to 47 ± 6 s and from 27 ± 21 s to 31 ± 2 s, respectively). The highest τ_2 of 60 ± 22 s was obtained for the "thin" film in contact with ES 2, but dropped dramatically in contact with the rougher substrates ES 3 and ES 4.

The pull-off stresses as a function of hold time, varied between 1 and 300 s, are displayed in Fig. 6. Unlike the "thick" films, the "thin" and the "medium" films showed a pronounced increase in pull-off stress with longer hold times. For "medium" films, the pull-off stress increased by a factor ranging from 1.7 to 3 per time decade (Fig. 6**b**); the "thin" films exhibited the highest sensitivity to the hold time, with a factor of 2.4–5 per time decade (Fig. 6**a**). In line with the results of Fig. 3, the sensitivity of the pull-off stress to the surface roughness decreased with increasing film thickness.

The results indicate that "thick" films are very insensitive to the hold time, while the adhesion of "thin" and "medium" films can be adjusted by varying the hold time. The rate of pull-off stress increase with time decreases at longer hold times, but a saturation could not be measured in our experiments. However, from the relaxation experiments (Fig. 5), we observe that the characteristic material relaxation time was between 27 and 60 s, the stress decrease being highest for the thickest films and yielding a plateau after less than 120 s. This indicates that the stress relaxation is not primarily influencing the pull-off stress increase at elongated hold times, as the influence of hold time is more pronounced for thinner films, and does not plateau, even after 300 s hold time.

4. Discussion

In this work, we presented adhesion measurements on epoxy substrates replicated from different surfaces, from polished glass to VitroSkin, an artificial model skin. Besides surface roughness, adhesion of two surfaces is fundamentally dependent on the surface free energy of the adhesive, substrate and interface between them (Packham, 2003). In order to be able to investigate the adhesion characteristics in relation to surface roughness only, the surface free energy of the substrate was kept constant by molding with epoxy in all cases.

The replicas exhibited slightly different roughness profiles compared to the original surfaces. This is most likely due to shrinkage of the epoxy resin during the curing process or to limited epoxy molding of fine asperities. However, we believe that this will not drastically influence the outcome of our study.

Adhesion measurements showed that, with increasing confinement, i.e. an increasing ratio between the punch diameter and the film thickness, the pull-off stress typically increases most likely because lateral retraction of the material is suppressed (Hensel et al., 2018). That explains the generally observed trend that the pull-off stress increased with decreasing film thickness. However, this is limited if the film thickness is in the same size scale as the mean peak to valley distance (R_z) of the substrates, as observed for epoxy substrates ES 3 and ES 4 for the thinnest film (Fig. 3**a**). Davis et al. discussed a material-defined length scale, δ_c, that describes the distance over which adhesive forces act and that qualitatively provides a measure of the critical size scale of surface roughness to impact adhesion (Davis et al., 2012). For confined elastic layers $\delta_c = \sqrt{G_c \cdot h_{film}/E}$, G_c and E being the critical energy release rate and the Young's modulus, respectively (Webber et al., 2003). This means that for a given adhesive material of a given thickness, there is a critical surface roughness parameter $R_{z,crit} = \delta_c$ above which the adhesion is strongly influenced by surface roughness. Conversely, for a given surface with roughness R_z there is a critical film thickness of the elastic material, $h_{film,crit} = R_z^2 \cdot E/G_c$, above which the adhesion will likely be insensitive to the surface roughness.

The lower bound of the critical energy release rate, under equilibrium conditions, equals the thermodynamic work of adhesion, typically about 50 mJ/m^2 for silicone materials. The Young's modulus of SSA 7–9800 is about 6 kPa as measured in our previous study assuming $E \approx 3 \cdot G$, G being the shear storage modulus measured at 0.01 Hz with a rheometer (Fischer et al., 2017b). Hence, $R_{z,crit}$ ranges between 22 µm and 52 µm, for the thin (h_{film} = 60 µm) and thick (h_{film} = 320 µm) films, respectively. These values are larger than R_z obtained from ES 1 and ES 2; this most probably explains why the surface topography does not affect the adhesion performance of all films. In contrast, $R_{z,crit}$ is in the same order than R_z of the substrate ES 3 and ES 4. Here, the surface asperities most likely have an impact on the adhesion performance related to strain energy distortions, particularly for the thinner films

(Fig. 3**a**). For the "thick" film, $R_{z,crit}$ is larger than R_z for all substrates, which likely indicates the small influence of the roughness on the adhesion measurements.

The apparent trend that the pull-off stresses seemed to be highest for the slightly rough substrate (ES 2), rather than for the smoothest substrate (ES 1) (Fig. 3**c**), requires further discussion. Unfortunately, the error bars are too large to make this an unambiguously significant observation. We note however that such a behaviour would be in line with earlier reports where similar effects of sub-micron roughness were found (Briggs and Briscoe, 1977; Purtov et al., 2013; Davis et al., 2012). For the "thin" films, the pull-off stress increased by about 25% compared to the smoothest substrate, which cannot be explained by the slight increase of real contact area. In fact, a soft elastic body adhering to a sub-micron rough substrate creates elastic strain distortions at the surface asperities, surrounded by regions with smaller strain distortions (Guduru and Bull, 2007). Guduru demonstrated that surface roughness resulted in a combination of stable and unstable crack growth: from the surface valleys, the crack moves continuously towards the top of asperities, where it is then hindered and requires higher stresses to continue to propagate, yielding dissipative zones for the small scale roughness (Guduru and Bull, 2007). This results in crack trapping, which leads to increased work of separation and higher pull-off stresses (Hui et al., 2004).

Contact time can have different superimposing effects on adhesion measurements, including stress relaxation in the material, defect annealing at the interface and development of chemical affinity at the interface. Stress relaxation experiments revealed that the characteristic relaxation times were much smaller than the hold times influencing the pull-off stresses in adhesion measurements. The stress relaxation reflects a combination of macroscopic and microscopic effects, i.e. a global deformation of the film due to the penetration of the punch and local deformation due to the surface asperities. Note that the indentation depth to achieve the pre-stress increased with increasing film thickness. Hence, bulk deformation most probably dominates the stress relaxation behaviour over microscopic defect annealing, particularly for film thicknesses much larger than R_z. For the thin films adhering to ES 3 and ES 4, where $h_{film} \approx R_z$, however, τ_2 varies as a function of the substrate, which likely indicates that the surface roughness affects the relaxation behaviour.

For "thick" films, we suggest that the low confinement yields stress concentrations at the edge of the contact zone, initiating detachment at the edge (Fig. 4). This detachment process is relatively independent of defects and defect annealing with increasing hold time. Both chemical affinity and stress relaxation seem to only marginally influence adhesion. For thin and medium-thick films, detachment is driven by stress concentrations within the contact area, influenced drastically by defects, yielding cavitation driven detachment. Thus, defect annealing at the interface contributes towards the increased adhesion strength observed.

5. Conclusions

We presented a study of the adhesion and material relaxation of a medical grade silicone SSA MG 7–9800. Substrate roughness, hold time and film thickness were varied and epoxy replicas from glass and VitroSkin substrates were used as counter surfaces. In this way, a description of the time-dependent interaction of soft elastomers on skin-like surfaces was provided. The following conclusions can be drawn:

- The adhesion behaviour of the thin films in our study was found to be very sensitive to surface roughness and hold time. Thicker films exhibited smaller pull-off stresses which were almost unaffected by roughness and hold time.
- Hold times improved adhesion only for the thinner films, which is very likely due to a combination of stress relaxation and defect annealing at the contact.
- Small surface roughness resulted in increased pull-off stresses; this is believed to indicate the occurrence of crack trapping.
- Thin films can achieve very high adhesion, also on rough surfaces, with the limitation that the film thickness must fulfil $h_{film} > R_z^2 \cdot E/G_c$, where E is the Young's modulus and G_c the critical energy release rate.

The results suggest that, for any application related to skin adhesion, the thickness of the adhesive layer should be judiciously chosen: While thick films provide smaller, but constant pull-off stresses, the adhesive behaviour of thinner films can be tuned with longer hold times. For the most versatile adhesives, thick layers should be chosen while thinner films achieve higher pull-off stresses on certain substrates.

Acknowledgements

The authors thank Costantino Créton (ESPCI Paris, France) and Martin Müser (Saarland University, Germany) for helpful discussions. Furthermore Martin Danner and Angela Rutz are acknowledged for their assistance in preparing samples. The authors would like to thank Biesterfeld Spezialchemie GmbH (Hamburg, Germany), especially Robert Radsziwill for continuous support and discussions. The research leading to these results has received funding from the European Research Council under the European Union's Seventh Framework Programme (FP/2007–2013) / ERC Grant Agreement n. 340929.

Authors contributions

All authors have contributed with conceptual design of the study. S.C.L.F., S.B. and K.K. performed the experiments and S.C.L.F. performed data analysis supported by S.B. All authors discussed the results and wrote the manuscript.

Competing financial interests

The authors declare no competing financial interests.

Appendix A. Supplementary material

Supplementary data associated with this article can be found in the online version at http://dx.doi.org/10.1016/j.jmbbm.2018.01.032.

References

Barreau, V., Hensel, R., Guimard, N.K., Ghatak, A., McMeeking, R.M., Arzt, E., 2016. Fibrillar elastomeric micropatterns create tunable adhesion even to rough surfaces. Adv. Funct. Mater. Mater. 26, 4687–4694. http://dx.doi.org/10.1002/adfm.201600652.

Briggs, G.A.D., Briscoe, B.J., 1977. The effect of surface topography on the adhesion of elastic solids. J. Phys. D. Appl. Phys. 10, 2453–2466. http://dx.doi.org/10.1088/0022-3727/10/18/010.

Castellanos, G., Arzt, E., Kamperman, M., 2011. Effect of viscoelasticity on adhesion of bioinspired micropatterned epoxy surfaces. Langmuir 27, 7752–7759. http://dx.doi.org/10.1021/la2009336.

Chen, S., Bhushan, B., 2013. Nanomechanical and nanotribological characterization of two synthetic skins with and without skin cream treatment using atomic force microscopy. J. Colloid Interface Sci. 398, 247–254. http://dx.doi.org/10.1016/j.jcis.2013.02.026.

Dapp, W.B., Lücke, A., Persson, B.N.J., Müser, M.H., 2012. Self-affine elastic contacts: Percolation and leakage. Phys. Rev. Lett. 108, 1–4. http://dx.doi.org/10.1103/PhysRevLett.108.244301.

Davis, C.S., Martina, D., Creton, C., Lindner, A., Crosby, A.J., 2012. Enhanced adhesion of elastic materials to small-scale wrinkles. Langmuir 28, 14899–14908. http://dx.doi.org/10.1021/la302314z.

Davis, C.S., Lemoine, F., Darnige, T., Martina, D., Creton, C., Lindner, A., 2014. Debonding mechanisms of soft materials at short contact times. Langmuir 30, 10626–10636. http://dx.doi.org/10.1021/la5023592.

Ferry, J.D., 1980. Viscoelastic properties of polymers.

Findley, W.N., Lai, J.S., Onaran, K., 2013. Creep and Relaxation of Nonlinear Viscoelastic Materials (January 15, 2013). Revised ed. Dover Publicationshttp://dx.doi.org/10.1604/9780486660165. (January 15, 2013).

Fischer, S.C.L., Arzt, E., Hensel, R., 2017a. Composite pillars with a tunable interface for adhesion to rough substrates. ACS Appl. Mater. Interfaces 9, 1036–1044.
Fischer, S.C.L., Kruttwig, K., Bandmann, V., Hensel, R., Arzt, E., 2017b. Adhesion and cellular compatibility of silicone-based skin adhesives. Macromol. Mater. Eng. 302, 1600526. http://dx.doi.org/10.1002/mame.201600526.
Fuller, K.N.G., Tabor, D., 1975. The effect of surface roughness on the adhesion of elastic solids. Proc. R. Soc. A Math. Phys. Eng. Sci. 345, 327–342. http://dx.doi.org/10.1098/rspa.1975.0138.
Greenwood, J.A., Williamson, J.B.P., 1966. Contact of Nominally Flat Surfaces. Proc. R. Soc. A Math. Phys. Eng. Sci. 295, 300–319. http://dx.doi.org/10.1098/rspa.1966.0242.
Guduru, P.R.R., Bull, C., 2007. Detachment of a rigid solid from an elastic wavy surface: experiments. J. Mech. Phys. Solids 55, 473–488.
Hensel, R., McMeeking, R.M., Kossa, A., 2018. Adhesion of a rigid punch to a confined elastic layer revisited. J. Adhes. http://dx.doi.org/10.1080/00218464.2017.1381603.
Hui, C.-Y., Glassmaker, N.J., Tang, T., Jagota, A., 2004. Design of biomimetic fibrillar interfaces: 2. Mechanics of enhanced adhesion. J. R. Soc. Interface 1, 35–48. http://dx.doi.org/10.1098/rsif.2004.0004.
Jacobs, T.D.B., Junge, T., Pastewka, L., 2017. Quantitative characterization of surface topography using spectral analysis. Surf. Topogr. Metrol. Prop. 5, 13001(doi:arXiv:1607.03040).
Jones, I., Currie, L., Martin, R., 2002. A guide to biological skin substitutes. Br. J. Plast. Surg. 55, 185–193. http://dx.doi.org/10.1054/hips.2002.3800.
Kenney, J.F., Haddock, T.H., Sun, R.L., Parreira, H.C., 1992. Medical-grade acrylic adhesives for skin contact. J. Appl. Polym. Sci. 45, 355–361. http://dx.doi.org/10.1002/app.1992.070450218.
Kim, T., Park, J., Sohn, J., Cho, D., Jeon, S., 2016. Bioinspired, highly Stretchable, and conductive dry adhesives based on 1D–2D hybrid carbon nanocomposites for all-in-one ECG electrodes. ACS Nano 10, 4770–4778. http://dx.doi.org/10.1021/acsnano.6b01355.
Krueger, E.M., Cullum, M.E., Nichols, T.R., Taylor, M.G., Sexton, W.L., Murahata, R.I., 2013. Novel instrumentation to determine peel force in vivo and preliminary studies with adhesive skin barriers. Skin. Res. Technol. 19, 398–404. http://dx.doi.org/10.1111/srt.12059.
Lakrout, H., Sergot, P., Creton, C., 1999. Direct observation of cavitation and fibrillation in a probe tack experiment on model acrylic pressure-sensitive-adhesives. J. Adhes. 69, 307–359. http://dx.doi.org/10.1080/00218469908017233.
Laulicht, B., Langer, R., Karp, J.M., 2012. Quick-release medical tape. Proc. Natl. Acad. Sci. USA 109, 18803–18808. http://dx.doi.org/10.1073/pnas.1216071109.
Lir, I., Haber, M., Dodiuk-Kenig, H., 2007. Skin surface model material as a substrate for adhesion-to-skin testing. J. Adhes. Sci. Technol. 21, 1497–1512. http://dx.doi.org/10.1163/156856107782844783.
Nase, J., Lindner, A., Creton, C., 2008. Pattern formation during deformation of a confined viscoelastic layer: from a viscous liquid to a soft elastic solid. Phys. Rev. Lett. 101, 074503. http://dx.doi.org/10.1103/PhysRevLett.101.074503.
Netzlaff, F., Lehr, C.-M., Wertz, P.W., Schaefer, U.F., 2005. The human epidermis models EpiSkin®, SkinEthic® and EpiDerm®: an evaluation of morphology and their suitability for testing phototoxicity, irritancy, corrosivity, and substance transport. Eur. J. Pharm. Biopharm. 60, 167–178. http://dx.doi.org/10.1016/j.ejpb.2005.03.004.
Packham, D., 2003. Surface energy, surface topography and adhesion. Int. J. Adhes. Adhes. 23, 437–448. http://dx.doi.org/10.1016/S0143-7496(03)00068-X.
Persson, B.N.J., Tosatti, E., 2001. The effect of surface roughness on the adhesion of elastic solids. J. Chem. Phys. 115, 5597. http://dx.doi.org/10.1063/1.1398300.
Purtov, J., Gorb, E.V., Steinhart, M., Gorb, S.N., 2013. Measuring of the hardly measurable: adhesion properties of anti-adhesive surfaces. Appl. Phys. A Mater. Sci. Process. 111, 183–189. http://dx.doi.org/10.1007/s00339-012-7520-3.
Putignano, C., Carbone, G., Dini, D., 2015. Mechanics of rough contacts in elastic and viscoelastic thin layers. Int. J. Solids Struct. 69–70, 507–517. http://dx.doi.org/10.1016/j.ijsolstr.2015.04.034.
Quan, M.B., Edwards, C., Marks, R., 1997. Non-invasive in vivo techniques to differentiate photodamage and ageing in human skin. Acta Derm. Venereol. 77, 416–419.
Renvoise, J., Burlot, D., Marin, G., Derail, C., 2009. Adherence performances of pressure sensitive adhesives on a model viscoelastic synthetic film: a tool for the understanding of adhesion on the human skin. Int. J. Pharm. 368, 83–88. http://dx.doi.org/10.1016/j.ijpharm.2008.09.056.
Tang, W., Zhang, J., Chen, S., Chen, N., Zhu, H., Ge, S., Zhang, S., 2015. Tactile perception of skin and skin cream. Tribol. Lett. 59, 24. http://dx.doi.org/10.1007/s11249-015-0540-3.
Tirella, A., Mattei, G., Ahluwalia, A., 2014. Strain rate viscoelastic analysis of soft and highly hydrated biomaterials. J. Biomed. Mater. Res. Part A 102, 3352–3360. http://dx.doi.org/10.1002/jbm.a.34914.
Tobin, D.J., 2006. Biochemistry of human skin—our brain on the outside. Chem. Soc. Rev. 35, 52–67. http://dx.doi.org/10.1039/B505793K.
Venkatraman, S., Gale, R., 1998. Skin adhesives and skin adhesion: 1. Transdermal drug delivery systems. Biomaterials 19. 〈http://www.sciencedirect.com/science/article/pii/S0142961298000209〉 (accessed 30 November 2014).
Webber, R.E., Shull, K.R., Roos, A., Creton, C., 2003. Effects of geometric confinement on the adhesive debonding of soft elastic solids. Phys. Rev. E. 68, 021805. http://dx.doi.org/10.1103/PhysRevE.68.021805.
Wokovich, A.M., Brown, S.A., McMaster, F.J., Doub, W.H., Cai, B., Sadrieh, N., Chen, M.L., Machado, S., Shen, M., Buhse, L.F., 2008. Evaluation of substrates for 90 degrees peel adhesion - A collaborative study. I. Medical tapes. J. Biomed. Mater. Res. Part B-Appl. Biomater. 87B, 105–113. http://dx.doi.org/10.1002/jbm.b.31075.